Carcinogenesis vol.20 no.3 pp.373–382, 1999

ACCELERATED PAPER

Effect of *hMSH6* cDNA expression on the phenotype of mismatch repair-deficient colon cancer cell line HCT15

Teresa Lettieri, Giancarlo Marra, Gabriele Aquilina[1], Margherita Bignami[1], Nigel E.A.Crompton[2], Fabio Palombo[3] and Josef Jiricny[4]

Institute of Medical Radiobiology, August Forel-Strasse 7, 8008 Zürich, Switzerland, [1]Istituto Superiore di Sanità, Viale Regina Elena 299, 00161 Rome, Italy, [2]Tumour Therapy Evaluation Laboratory, Paul Scherrer-Institute, 5232 Villigen, Switzerland and [3]Istituto di Ricerche di Biologia Molecolare 'P.Angeletti', Via Pontina km 30 600, I-00040 Pomezia, Italy

[4]To whom correspondence should be addressed
Email: jiricny@imr.unizh.ch

Mismatch recognition in human cells is mediated primarily by a heterodimer of hMSH2 and hMSH6. Cells mutated in both alleles of the *hMSH6* gene are deficient in the correction of base/base mispairs and insertion/deletion loops of one nucleotide and thus exhibit a strong mutator phenotype, evidenced by elevated mutation rates and microsatellite instability, as well as by tolerance to methylating agents. The decrease in replication fidelity associated with a loss of mismatch correction implies that with each division, these cells are likely to acquire new mutations throughout their genomes. Should such secondary mutations occur in genes linked to replication fidelity or involved in the maintenance of genomic stability, they might contribute to the observed mutator phenotype. The human colon tumour line HCT15 represents one such case. Although it carries inactivating mutations in both *hMSH6* alleles, it has also been shown to contain a missense mutation in the coding sequence of the proofreading domain of the polymerase-δ gene. In an attempt to find out whether the phenotype of HCT15 cells was indeed brought about solely by the lack of hMSH6, we stably transfected them with a vector carrying the wild-type *hMSH6* cDNA. Our results show that although the levels of transgenic hMSH6 were low, expression of the wild-type protein resulted in a substantial restoration of mismatch binding, mismatch repair capacity and the stability of mononucleotide repeats, as well as in the reduction of mutation rates. Although methylation tolerance of the hMSH6-expressing cells was not markedly affected, the G_2 cell cycle checkpoint, absent in *N*-methyl-*N*′-nitro-*N*-nitrosoguanidine-treated control cells, was restored.

Introduction

Mutations in genes encoding mismatch repair proteins have been found in both sporadic and hereditary colon cancers (1–4). Post-replicative mismatch correction increases the fidelity of DNA replication by up to three orders of magnitude in all organisms studied to date (5). Cells deficient in mismatch repair display elevated spontaneous mutation frequencies, instability of repeated sequence motifs (e.g. microsatellites), increased gene conversion and recombination levels (4,6,7) and tolerance to certain types of DNA-modifying drugs (8). Our understanding of this repair pathway in human cells has been greatly facilitated by the fact that the process is highly conserved throughout evolution. Thus, genetic and biochemical studies of mismatch repair in lower organisms, in particular *Escherichia coli* and *Saccharomyces cerevisiae*, have been extremely informative. Moreover, the different phenotypes of human tumour-derived mismatch repair-deficient cells helped to elucidate the roles of the individual mismatch repair proteins in the correction process. Biochemical studies carried out with extracts of these cells were instrumental in the discovery that, while in *E.coli* the initial steps of mismatch correction are mediated by the homodimeric MutS and MutL proteins, recognition of base/base mispairs and small insertion/deletion loops (IDLs) in human extracts is mediated primarily by hMutSα, an abundant heterodimer of two MutS homologues, hMSH2 and hMSH6 (the latter is also known as GTBP or p160) (9–11). The resulting protein–DNA complex is subsequently bound by a second heterodimer, hMutLα, composed of hMLH1 and hPMS2 (12). The system also appears to have some built-in redundancy, as a second heterodimer, hMutSβ, composed of hMSH2 and hMSH3, participates in the correction of IDLs, but not base/base mispairs (13–16).

There is little doubt that inheritance of mutations in mismatch repair genes, especially in *hMLH1* and *hMSH2*, predisposes to cancer of the colon, endometrium and ovary, as witnessed by the high frequency of these types of tumours in hereditary non-polyposis colon cancer (HNPCC) families (2). Indeed, the discovery that tumour tissue from HNPCC patients exhibited microsatellite instability, a phenotype referred to as replication error in repeats (RER^+) (17), instigated the search for defects in DNA replication or post-replicative repair. There is also ample evidence that the RER^+ phenotype, elevated mutation frequency, mismatch repair deficiency and tolerance to methylating agents are linked with mutations in mismatch repair genes (3,4,18). However, unambiguous evidence that these mutations are entirely responsible for the observed phenotype is still lacking. This is due to the fact that mismatch repair-deficient cells have a propensity to acquire new mutations during each replication cycle. The possibility that such mutations could have arisen in other genes involved in the maintenance of genomic integrity could therefore not be excluded. A case in point is the human colon tumour line HCT15. These cells carry a mutated *hMSH6* gene, with one allele having been inactivated by a single nucleotide deletion mutation in codon 222 which results in a change from leucine to a termination codon and the other allele having a complex deletion/substitution mutation (GATAGA→T) at codon 1103, which causes protein synthesis to terminate three amino acid

Abbreviations: BrdU, 5-bromo-2′-deoxyuridine; DMEM, Dulbecco's modified Eagle's medium; DMSO, dimethylsulphoxide; DTT, dithiothreitol; HNPCC, hereditary non-polyposis colon cancer; HU, hydroxyurea; IDL, insertion/deletion loop; MGMT, O^6-methylguanine methyltransferase; MNNG, *N*-methyl-*N*′-nitro-*N*-nitrosoguanidine; MNU, *N*-methyl-*N*-nitrosourea; PBS, phosphate-buffered saline; PMSF, phenylmethylsulphonyl fluoride; pol, polymerase; RER, replication error in repeats; 6-TG, 6-thioguanine.

residues downstream (19). HCT15 cells are, correspondingly, defective in the correction of base/base mismatches and small IDLs, as measured by an *in vitro* assay (9), and have a strong mutator phenotype (20,21). They are also tolerant to high concentrations of methylating agents (22). However, an earlier study also identified a mutation in the polymerase (pol)-δ gene, where a G→A transition mutation alters a conserved amino acid residue that is located in the 3′→5′ proofreading exonuclease domain of the protein (23). As mutations in the proofreading exonuclease subunits of other polymerases are known to possess extremely strong mutator phenotypes (24), there exists the possibility that the pol-δ mutation contributes to the phenotype of HCT15 cells. One way to answer this question is to express the wild-type hMSH6 protein in these cells and to see whether the mutator phenotype of the transfected cells has been corrected. We now report that expression of wild-type hMSH6 in HCT15 cells resulted in a substantial correction of the defects in mismatch binding and base/base mispair correction and restored stability to microsatellite sequences. Although expressed only at low levels, wild-type hMSH6 also brought about a modest reduction in mutation rate at the *HPRT* locus. The sensitivity of the hMSH6-expressing HCT15 cells to methylating agents remained largely unaltered, but the G_2 cell cycle checkpoint, which is generally absent from mismatch repair-deficient cells following treatment with methylating agents (25), appears to have been restored.

Materials and methods

The reagents used in these experiments were obtained from the following sources: pCDNA-3 from Invitrogen (San Diego, CA); G418 (Geneticin) from Gibco BRL Life Technologies (Gaithersburg, MD). *N*-methyl-*N*-nitrosourea (MNU; Sigma, St Louis, MO) was dissolved in dimethylsulphoxide (DMSO) and diluted in phosphate-buffered saline (PBS)/20 mM HEPES, pH 7.4, to the required concentration immediately before use. A stock solution of O^6-benzylguanine (a kind gift of J.Thomale, University of Essen, Essen, Germany) was prepared in DMSO and stored at –20°C. The Megaprime DNA labelling system was from Amersham International (Little Chalfont, UK); Dulbecco's modified Eagle's medium (DMEM) was from Gibco; the HCT15 cell line was kindly provided by Dr Thomas Kunkel (NIEHS, NC). Standard laboratory procedures were carried out according to Sambrook *et al*. (26).

Construction of the hMSH6 cDNA expression vector

The full-length *hMSH6* cDNA (10,27) was excised from plasmid pBluescript hMSH6 (10) with *Bam*HI and *Xho*I. The 4283 bp fragment was ligated between the *Bam*HI and *Xho*I sites of pCDNA-3. The resulting plasmid, pCDNA/hMSH6, and the control, insert-less pCDNA-3 vector were purified by isopycnic centrifugation on a CsCl gradient and transfected into HCT15 cells. The insert in the H-5 clone was then sequenced to ensure that no mutations were present in the *hMSH6* coding region.

Transfection of HCT15 cells and selection of stable clones

The HCT15 cells were grown in DMEM supplemented with 10% fetal bovine serum (Gibco), in a humidified 5% CO_2 atmosphere at 37°C. The DNA transfection of HCT15 cells was performed by the calcium phosphate precipitation technique. Briefly, logarithmically growing cells were subcultured at a density of 1×10^6 cells/10 cm dish and 24 h later 20 μg plasmid DNA/calcium phosphate precipitate were left on the cells overnight. The cells were washed and incubated for 2 days in fresh culture medium, whereupon selection was initiated by the addition of G418 to the growth medium at 900 μg/ml. After 3 weeks, the resistant colonies were collected in cloning rings and propagated into mass cultures. Three weeks later, the colonies were analysed for hMSH6 expression. The clones stably expressing hMSH6 were maintained in a medium containing 900 μg/ml G418. One clone, named H-5, expressing the highest level of hMSH6 (see below), was selected for further study. A second clone, named H-c, stably transfected with the empty expression vector, was used as a control.

Preparation of nuclear extracts

Nuclear extracts were prepared according to the method of Dignam *et al*. (28). The harvested cells were washed twice with PBS, collected and dissolved in 1 vol ice-cold buffer A [10 mM HEPES, pH 7.9, 10 mM KCl, 1.5 mM $MgCl_2$, 1 mM dithiothreitol (DTT), 1 mM phenylmethylsulphonyl fluoride (PMSF)]. After 15 min incubation on ice, the cells were homogenized with 15 strokes in a glass micro-Dounce homogenizer pre-rinsed with buffer A. The homogenate was centrifuged in an Eppendorf microfuge for 20 s at 12 000 r.p.m. The nuclear pellets were resuspended in two-thirds vol ice-cold buffer C (20 mM HEPES, pH 7.9, 420 mM NaCl, 1.5 mM $MgCl_2$, 0.2 mM EDTA, 20% glycerol, 1 mM DTT, 1 mM PMSF) and incubated for 30 min at 4°C on a rotating wheel. The samples were then centrifuged for 5 min at 12 000 r.p.m. and the supernatant was collected, snap frozen in small aliquots in liquid nitrogen and stored at –80°C.

Band shift assays

The band shift assays were carried out as described previously (29). Briefly, ^{32}P-labelled 34mer oligonucleotide duplexes, either perfectly matched (G/C) or containing a single G/T mismatch (G/T), were incubated with 15 μg nuclear extract in the presence of 25 mM HEPES–KOH, pH 8.0, 0.5 mM EDTA, 10% (v/v) glycerol, 0.5 mM DTT and 1 μg poly(dI·dC) competitor DNA (Boehringer Mannheim, Mannheim, Germany) in a total volume of 20 μl. The mixture was allowed to stand at room temperature for 20 min. Five microliters of the mixture were loaded onto a 6% non-denaturing polyacrylamide gel run in 1× TAE buffer. Electrophoresis was carried out at 150 V until the bromophenol blue dye, loaded in an adjacent well, migrated ~7 cm. The dried gels were autoradiographed at –80°C.

Immunoblotting (western) analysis

Aliquots of 25–100 μg nuclear extract were loaded on 7.5% SDS–polyacrylamide gels. After electrophoresis, the proteins were transferred to a nitrocellulose membrane (Schleicher & Schuell) by electroblotting at 30 V overnight at 4°C in 25 mM Tris, 192 mM glycine and 20% methanol. The membrane was blocked with 5% low fat milk in TBST (100 mM Tris–HCl, pH 8, 150 mM NaCl, 0.05% Tween 20) for 1 h at room temperature. The membrane was then incubated for 1 h at room temperature with mouse monoclonal anti-hMSH6 (15) and anti-hMSH2 (AB-2; Calbiochem) antibodies at a final concentration of 0.8 and 0.2 μg/ml, respectively. After three washes with TBST, the membrane was incubated with alkaline phosphatase-conjugated anti-mouse IgG (1:4000; Sigma) for 1 h at room temperature and developed according to the manufacturer's (Sigma) instructions.

Northern blot analysis

Total RNA was extracted from logarithmically growing HeLa, H-c and H-5 cells with TRIzol reagent (Gibco BRL). Aliquots of 30 μg were then suspended in formamide loading buffer and electrophoresed on a 1% formaldehyde–agarose gel. The positions of the 28S and 18S rRNAs were determined by inspection on a UV transilluminator and the gel was then blotted for 16 h in 20× SSC on a Genescreen nylon membrane (DuPont/NEN, Keene, NH). The filter was rinsed in 2× SSC, baked under vacuum for 1 h at 80°C and crosslinked for 30 s in a Stratalinker (Stratagene, La Jolla, CA). Prehybridization was performed in 5× SSPE, 50% formamide, 5× Denhardt's solution, 1% SDS, 10% dextran sulphate and 100 mg/ml denatured salmon sperm DNA for 2 h at 42°C. Hybridization was carried out in the same buffer containing 1×10^6 c.p.m./ml ^{32}P-labelled random primed 2 kb gel-purified *hMSH6* fragment for 16 h at 42°C. The membrane was washed once at room temperature in 2× SSPE (10 min), once at 65°C in 2× SSPE, 2% SDS (10 min) and the filter was then air dried and autoradiographed.

RT–PCR analysis of hMSH6 expression in HeLa, H-c and H-5 cells

hMSH6 cDNA was synthesized by reverse transcription, starting from 4 μg total RNA. Following denaturation by heating for 5 min at 75°C, a mixture containing 100 pmol oligo $d(T)_{12–18}$ primer (Pharmacia Biotech, Uppsala, Sweden) and 1000 U Moloney murine leukaemia virus reverse transcriptase (M-MLV 200 U/μl; Promega, Madison, WI) in 20 μl 10 mM DTT, 50 mM Tris–HCl, pH 8.3, 75 mM KCl, 3 mM $MgCl_2$ and 0.2 mM each deoxynucleoside triphosphate (Pharmacia Biotech) was added and the reaction was incubated for 1 h at 37°C. The enzyme was inactivated by heating for 5 min at 95°C. The PCR primers pT7 (TAATACGACTCACTATAGGG), C15r (AACTGTACATGAACACGGA) and Nick5 (CGGGATCCGATGTCGCGACAGAGCACC; Figure 1a) were then used to amplify the *hMSH6* transcripts. PCR was performed using 35 cycles of 95°C for 1 min, 50°C for 45 s and 72°C for 90 s in 1× buffer (Stratagene) with 100 ng HeLa cDNA or with 50 ng H-c or H-5 cDNA, 5% DMSO, 0.2 mM each deoxynucleoside triphosphate, 1 mM each primer and 2.5 U Taq polymerase (Taq-plus Precision PCR System; Stratagene). The products were separated by electrophoresis in an agarose gel containing ethidium bromide and visualized on a UV transilluminator (Figure 1c).

Mutation rate analysis

The H-c and H-5 cells were plated at low density (100 cells/dish) to ensure the absence of pre-existing mutants. The cultures were grown to between 5×10^4 and 1.5×10^6 cells/dish. All cells in each replicate were plated into

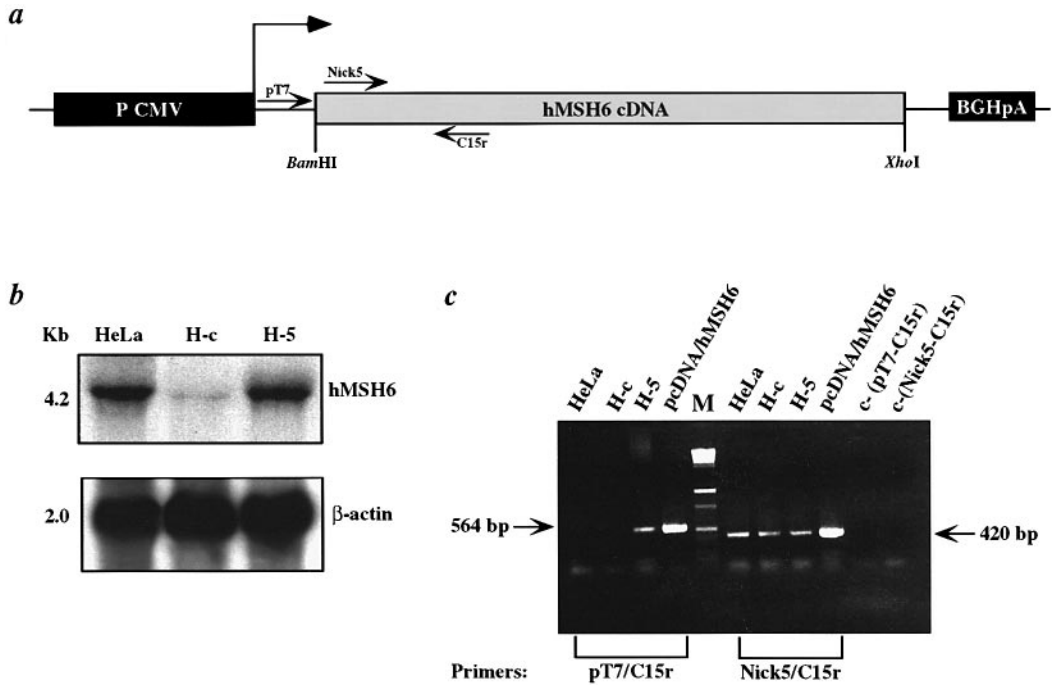

Fig. 1. Northern blot and RT–PCR analysis of hMSH6 expression in H-5 cells. (**a**) Schematic representation of the retroviral expression vector. P CMV, enhancer/promoter cassette of cytomegalovirus; BGHpA, bovine growth hormone polyadenylation signal sequence. Arrows indicate the position and orientation of primers used in the RT–PCR experiments. The dashed arrow indicates the transcription start site. (**b**) Hybridization of total RNA extracted from HeLa, H-c and H-5 cells with either a radiolabelled *hMSH6* probe (top) or with a reference β-actin probe (bottom). (**c**) RT–PCR analysis of hMSH6 expression. Amplification of *hMSH6* cDNA reverse transcribed from total mRNA isolated from HeLa, H-c and H-5 cells. PCR reactions with the primer pair Nick5/C15r amplified both endogenous and transgenic *hMSH6* cDNA. In contrast, only transgenic cDNA was amplified with the primer pair pT7/C15r [see (a)]. Plasmids pCDNA and pCDNA/hMSH6 were used as controls. In the two right-most lanes are the negative controls, where the amplification reactions were carried out with both primer pairs in the absence of DNA.

selective medium containing 6-thioguanine (6-TG; Sigma) at a density $\leqslant 5\times10^5$ cells/10 cm dish. Colonies were grown for 2 weeks before fixing with methanol and staining with 10% Giemsa in aqueous solution. Only colonies with >50 cells were counted. Mutation rates were calculated by the method of the mean (20).

DNA sequence analysis of HPRT mutations

H-c and H-5 cells were plated at a density of 100 cells/dish and grown to a final number of 5×10^5 cells. The replica cultures were trypsinized and plated in 6-TG at a density of 125×10^3 cells/10 cm dish. After 2 weeks, the colonies were picked with cloning cylinders and grown to confluence in 24-well tissue culture plates. RNA was isolated from the $HPRT^-$ mutants with TRIzol reagent. The mutant RNAs were reverse transcribed as described above using a *HPRT* primer complementary to the 3′-end of the non-coding region (GTTTCCAAACTCAACTTGAACTCTC). The cDNA products were amplified using a second primer (CCGGCTTCCTCCTCCTGAGC) complementary to the 5′-end of the gene. The PCR products were purified and sequenced with nested primers according to the ABI PRISM dRhodamine terminator cycle sequencing reaction kit (Perkin Elmer/Applied Biosystems, Wilton, CT). In mutants displaying loss of exons from the cDNAs, genomic DNA was extracted by standard methods and the exon–intron boundaries were PCR amplified with specific primers. The sequencing reactions were performed with nested primers.

Mismatch repair assays

The efficiency of cytoplasmic extracts of the stably transfected cells in repairing DNA mismatches was tested as described previously (15). Briefly, cytoplasmic extracts were prepared from 5×10^8 HeLa, parental HCT15, H-c and H-5 cells harvested in the logarithmic growth phase. Following resuspension in an appropriate volume of ice-cold hypotonic buffer to yield a cell density of 1×10^8 cells/ml, the cells were allowed to swell for 10 min in a glass Dounce homogenizer (Kontes, Vineland, NJ) on ice and then lysed mechanically with four or more strokes with a tight (type B) pestle. When >80% of cells were lysed, the nuclei were pelleted and the supernatant was centrifuged at 12 000 *g* for 10 min at 4°C, frozen in liquid nitrogen in aliquots and stored at –80°C. The protein concentration was determined by the Bradford method (30). M13mp2 DNA heteroduplexes containing a G/G, G/T or T/G base mispairs in the coding sequence of the *lacZ* α-complementation gene were obtained by hybridizing single-stranded viral (+) DNA with the (–) strand of linearized RF DNA. One femtomole of the respective heteroduplex was used in a repair reaction (25 µl) with 30 mM HEPES, pH 7.8, 7 mM $MgCl_2$, 4 mM ATP, 200 µM each CTP, GTP and UTP, 100 µM each dATP, dGTP, dTTP and dCTP, 40 mM creatine phosphate, 100 fmol creatine phosphokinase, 15 mM sodium phosphate, pH 7.5, and 50 µg protein extract. The incubation was carried out at 37°C for 20 min. The repair was directed to the (–) strand of M13mp2 by the presence of a nick. The DNA heteroduplex was then purified and introduced by electroporation into *Escherichia coli* NR9162 (*mutS* strain), plated on minimal medium in a soft agar layer containing 0.5 ml of a log phase culture of CSH50 (the α-complementation strain), 0.5 µg isopropyl-β-D-thiogalactopyranoside and 2 µg 5-bromo-4-chloro-3-indoyl-β-D-galactopyranoside. Following incubation for 16 h at 37°C, the plaques were assigned to one of the following phenotypes: blue, colourless or mixed. If no repair occurred, mixed plaques were observed containing both blue and colourless progeny. Repair of the substrate reduced the percentage of mixed plaques and increased the percentage of pure colour plaques. As the nick directs repair to the (–) strand, the (+) phenotype increases and the (–) phenotype decreases.

Microsatellite analysis

A 121 bp region encompassing 26 deoxyadenosines localized in an intron of *hMSH2* (BAT26) was amplified by PCR using 4,7,2′,7′-tetrachloro-6-carboxyfluorescein-labelled forward primer 5′-TGACTACTTTTGACTT-CAGCC-3′ and reverse primer 5′-AACCATTCAACATTTTTAACCC-3′ (300 nM each). The amplification was carried out in 25 µl total volume with GenAmp 1× PCR buffer (Perkin Elmer), 1.25 U AmpliTaq Gold DNA polymerase (Perkin Elmer), 1.5 mM $MgCl_2$, 100 µM deoxynucleotide triphosphates and 5 ng genomic DNA extracted from each single cell clone. After 1 cycle of 94°C for 9 min to activate AmpliTaq DNA polymerase, 30 cycles of 94°C for 45 s, 51°C for 1 min and 70°C for 30 s and a final elongation step at 70°C for 7 min were performed. Mock reactions without DNA were performed with every twentieth sample and were always negative. After dilution, the PCR products were denatured with formamide at 92°C for 2 min and electrophoresed through a polymer capillary in an ABI PRISM 310 Genetic Analyzer (Perkin Elmer). The sizing and quantitation of the DNA fragments was performed with the GenScan Analysis software (Perkin Elmer).

Methylation tolerance studies

This experiment was carried out as described previously (31). To measure cell survival, 100 cells were treated 18 h after seeding in 6 cm dishes for

30 min at 37°C with various concentrations of MNU in PBS/20 mM HEPES, pH 7.4. Cells were then washed, fed with complete medium and, 1–2 weeks later, the surviving colonies were fixed with methanol, stained with Giemsa and counted. In the experiments performed in the presence of O^6-benzylguanine, the drug was added to the medium at a final concentration of 25 μM 2 h prior to the MNU treatment and kept in the medium for an additional 72 h.

Cell cycle analysis

Cell synchronization in early S phase was accomplished by treatment with hydroxyurea (HU; Sigma). Confluent cells arrested in the resting phase were replated in fresh complete medium along with 2 mM HU to allow G_1 traverse. Fourteen hours later, by which time all cells had accumulated in early S phase, the HU was removed by two washes with prewarmed serum-free medium. The cells were then treated with 0 or 5 μM *N*-methyl-*N*′-nitro-*N*-nitrosoguanidine (MNNG; Sigma) in serum-free medium for 45 min at 37°C and 5% CO_2. After treatment, they were washed once with 10% serum-containing medium and returned to drug-free 10% serum-containing medium for 2, 4.5, 7, 12, 15 and 19 h. At each time point, the cells were incubated with 10 μM 5-bromo-2′-deoxyuridine (BrdU; Sigma) for 30 min before harvesting. They were then washed with PBS, fixed in 70% ethanol and stored at 4°C. Nuclear preparation and dual labelling of DNA by propidium iodide (Sigma) and anti-BrdU–fluorescein conjugate (Boehringer Mannheim, Basel, Switzerland) were performed as described (25). Cell cycle analysis was performed using a Becton Dickinson (Lincoln Park, NJ) FACscan flow cytometer and Cell Quest software. The data analysis is based on two independent experiments.

Results

Stable transfection of HCT15 cells with a retroviral vector carrying the hMSH6 cDNA results in the expression of hMSH6 *mRNA*

The expression vehicle pCDNA-3 is an integrating retroviral vector containing a selectable marker gene that confers resistance to G418. The *hMSH6* cDNA was cloned between the cytomegalovirus enhancer/promoter cassette and a polyadenylation signal sequence of the human growth hormone gene. The correct orientation of the insert was ensured by directional cloning between *Bam*HI and *Xho*I sites of the vector (Figure 1a; see also Materials and methods).

The *hMSH6* expression vector pCDNA/hMSH6 was transfected into logarithmically growing HCT15 cells by calcium phosphate precipitation. Following long-term selection for G418 resistance, a total of 10 clones were obtained, which were selected and grown into mass cultures under constant selective pressure. These clones were tested for the presence of integrated *hMSH6* cDNA by Southern blotting, as well as for expression of the protein by band shift and immunoblotting assays. Of these 10 clones, two, H-2 and H-5, contained detectable amounts of *hMSH6* cDNA. We selected clone H-5 for further analysis. Southern blot experiments indicated that H-5 carries about three copies of the integrated vector DNA (data not shown).

Because the H-5 clone was resistant to G418, the selectable marker gene was clearly expressed from the transfected vector. We therefore decided to test whether this clone also expressed *hMSH6* mRNA. To this end, total RNA isolated from HeLa, H-c (control, HCT15 cells stably transfected with the empty pCDNA-3 vector) and H-5 cells was size fractionated on an agarose gel, transferred to a nitrocellulose membrane and hybridized with a radiolabelled *hMSH6* probe as described in Materials and methods. The relative quantities of the specific signals were normalized with respect to β-actin. As shown in Figure 1b, the amount of *hMSH6* mRNA in the H-5 clone corresponded to ~50% of that seen in HeLa cells. In contrast, the H-c clone expressed only low amounts of *hMSH6* mRNA. It is possible that the *hMSH6* promoter is epigenetically inactivated in the H-c cells. However, we consider it more likely that the mRNA is selectively degraded due to the

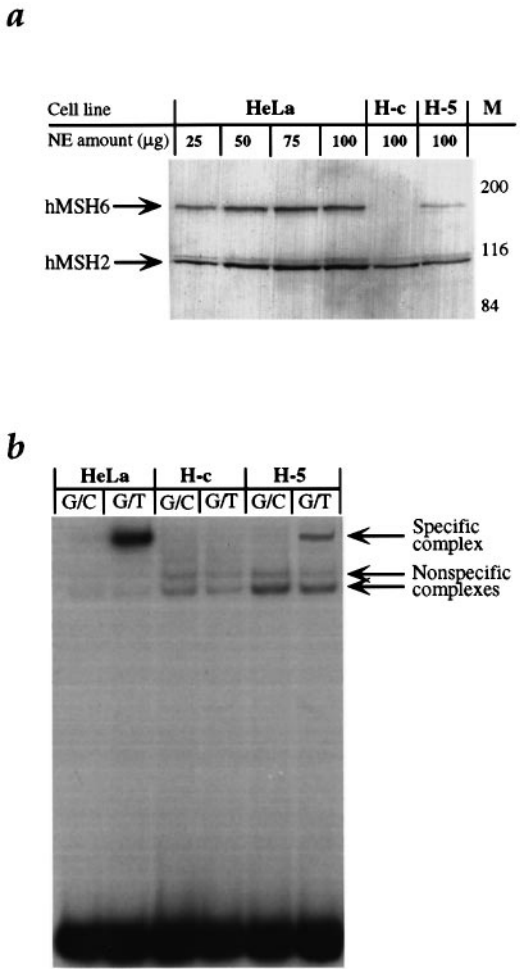

Fig. 2. (**a**) Immunoblot analysis of HeLa, H-c and H-5 extracts. Monoclonal antisera to hMSH6 and hMSH2 recognized bands of 160 and 100 kDa, respectively. Aliquots of 100 μg H-c and H-5 extracts were loaded. Aliquots of 25–100 μg HeLa extract were loaded in order to aid in quantitation of the hMSH6 signal observed in the transfected cell extracts. M, molecular size markers (Bio-Rad, Hercules, CA). (**b**) Mismatch binding activity in extracts of H-c and H-5 cells. The extracts were incubated with radioactively labelled oligonucleotide duplexes either complementary (G/C) or containing a single G/T mispair (G/T, see Materials and methods). The G/T-specific complex was absent in H-c extracts that lack hMSH6, but was restored upon expression of hMSH6 in H-5 cells. The extract of mismatch repair-proficient HeLa cells was used as a control.

presence of the premature termination codons (32). This result indicates that the 4.2 kb signal seen in the stably transfected clone H-5 is due almost entirely to the transcript originating from the transgene. We could substantiate this prediction further by the RT–PCR experiments shown in Figure 1c. Using two primer pairs, one specific for the RNA expressed from the transgene and one generic (Figure 1a, primers pT7/C15r and Nick5/C15r, respectively), we could show that while a fragment of 420 bp was obtained following RT–PCR of all three lines (Figure 1a, lanes Nick5-C15r), a transgene-specific signal was visible solely in the H-5 clone (Figure 1a, lanes T7-C15r). This result conclusively proved that the *hMSH6* transcript originated from the integrated expression vector.

Expression of hMSH6 in H-5 cells restores mismatch binding activity

Western blotting experiments confirmed that the *hMSH6* transcript was also translated, as the extracts of the H-5 clone contained hMSH6 (Figure 2a). In extracts of mismatch repair-

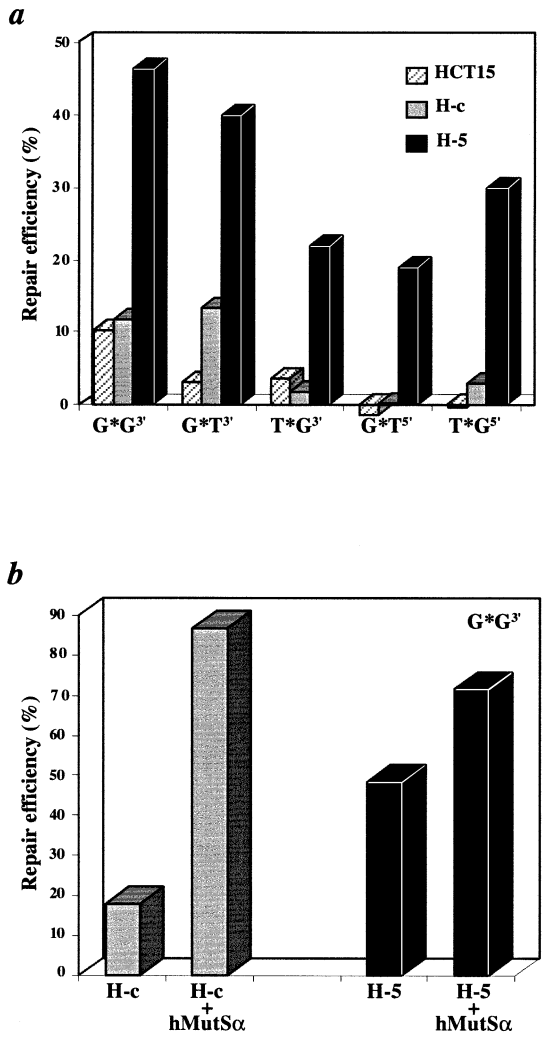

Fig. 3. Mismatch repair assays. (**a**) Correction efficiency of the G/T, T/G and G/G M13mp2 heteroduplex substrates, carrying a strand discrimination signal either 5′ or 3′ from the mispair. (**b**) Complementation of H-c and H-5 extracts with purified recombinant hMutSα.

proficient cells, such as HeLa shown in this example, the hMSH2 and hMSH6 proteins are present in a 1:1 ratio, while the extracts of H-c cells contained only hMSH2 in detectable amounts (10). Quantification of the immunoblot revealed that the amount of hMSH6 in H-5 extracts was only ~20% of the hMSH2 level. These extracts therefore contain about five times less hMutSα than HeLa cells.

The band shift assay shown in Figure 2b revealed that nuclear extracts of H-5 cells contained a mismatch-specific DNA binding activity, with a mobility similar to that present in extracts of HeLa cells, while no similar protein–DNA complex was present in the extracts of the control clone, H-c. We therefore assigned the mismatch-specific activity to hMutSα.

H-5 extracts are proficient in mismatch repair

The extracts of H-5 and H-c cells were tested for mismatch correction efficiency *in vitro*, using circular M13 heteroduplex substrates carrying either the G/T, T/G or G/G mispairs and strand directional signals (nicks) either 5′ or 3′ from the mispairs (see Materials and methods). As shown in Figure 3a, mismatch repair was restored in the H-5 extracts, with all substrates having been corrected to a level at least 5-fold above background. This repair capacity was relatively low, however, especially when compared with HeLa extracts, which typically repair >90% of the substrate in this assay (data not shown). We therefore decided to test whether this reduced repair capacity was due solely to the low levels of hMSH6 expression or whether the extracts were of poor quality. To this end, we added recombinant hMutSα to the extracts and determined if this improved the repair efficiency. As shown in Figure 3b, complementation of repair-deficient extracts of HCT15 and H-c cells resulted in the correction of nearly 90% of the G/G substrate. A substantial improvement was also observed in the H-5 extracts, which indicated that the repair capacity of these extracts was limited by the quantity of hMutSα. Taken together, the results of the western blotting, band shift and *in vitro* mismatch repair experiments all showed that the amount of hMutSα expressed in H-5 cells is limiting.

Table I. Microsatellite instability of the BAT26 locus of H-c and H-5 cells

Cell line	Stable clones	Unstable clones
H-c	67	23
H-5	84	5

Table II. Mutation rates at the *HPRT* locus of H-c and H-5 cells

Cell line	Initial cell no.	Final cell no.	No. of replica cultures	Mutant colonies (mean×no.)	Mutation rate
H-c	100	$1.05+\times10^{6}$	23	158 ± 0.6	2.5×10^{-5}
H-5	100	$1.15+\times10^{6}$	23	55 ± 11	0.8×10^{-5}
H-c:H-5 ratio				3.1	

Microsatellite instability is alleviated in the H-5 clone

Despite the low protein levels, we decided to test whether expression of hMSH6 in the H-5 clone affected the microsatellite instability of these cells. We decided to use the BAT26 marker, which targets a repeat of 26 adenines and has been shown to be exquisitely sensitive to mutations in *hMSH6* (19). Analysis of 90 H-c and 89 H-5 clones showed that expression of hMSH6 in HCT15 cells was sufficient to greatly alleviate microsatellite instability (Table I). Thus, while 23 of the examined H-c clones displayed instability at this locus, only five H-5 clones did. This difference is highly statistically significant ($P = 0.0002$). All mutations detected were deletions of a further nucleotide in the already shortened BAT26 poly(A) microsatellite of the HCT15 cells.

Mutation rate is decreased in H-5 cells

HCT15 cells display a strong mutator phenotype. Mutation rate measured at the *HPRT* locus is elevated ~200- to 600-fold as compared with mismatch repair-proficient cells (21,33). We therefore determined the mutation rate at this locus for the H-c and H-5 clones. The data shown in Table II indicate that expression of hMSH6 in HCT15 cells did indeed reduce the mutation rate, albeit only ~3-fold.

Although this reduction might appear of little significance, sequencing of the mutated *HPRT* cDNA revealed that the mutation spectra of the control and the H-5 cells were different (Table III). Thus, while transition, transversion and frameshift mutations represented 33, 45 and 12% of changes observed in the mutated *HPRT* gene of the control cells, the H-5 line

Table III. Spontaneous mutation spectra of the *HPRT* locus of H-c and H-5 cells

	H-c	H-5
Mutations characterized	24	26
Transitions	8 (33%)	4 (15%)
A:T→G:C	4	2
G:C→A:T	4	2
Transversions	11 (45%)	17 (65%)
G:C→T:A	8	14
G:C→C:G	0	1
T: A→A:T	3	0
A:T→C:G	0	2
Frameshifts	3 (12%)	1 (4%)
Deletions	0	4 (15%)
Undefined mutations	2 (8%)	0

Table IV. Progression of the untreated or MNNG-treated H-c and H-5 cells through the cell cycle after release from an HU block

Cell cycle phase	Time post-release (h)	H-c (%)	H-c/MNNG (%)	H-5 (%)	H-5/MNNG (%)
G_1	2	1.7	12.5	6.1	16.7
	4.5	4.1	8.7	1.8	7.7
	7	6.1	10.1	1.9	3.7
	9	10.4	4.6	8.9	5.8
	12	12.1	13.2	12.9	4.5
	15	41.1	36.1	36.1	9.7
	19	22.9	24.6	12.8	22.1
S	2	97.8	86.8	93.3	78.5
	4.5	93.9	88.2	97.4	87.3
	7	64.4	67.9	72.2	91.3
	9	34.5	42.3	37.5	79.6
	12	12.1	30.1	9.1	76.9
	15	53.1	43.3	54.9	55.1
	19	71.4	72.5	80.4	46.6
G_2/M	2	0.5	0.7	0.5	4.8
	4.5	1.9	3.1	0.7	4.9
	7	29.6	22.1	25.9	4.9
	9	55.1	53.1	53.6	14.6
	12	75.8	56.7	78.1	18.6
	15	5.9	20.5	8.9	35.2
	19	5.7	2.8	6.7	31.4

displayed primarily transversions and deletions of multiple bases. Transitions and frameshifts, which arise from uncorrected purine/pyrimidine mispairs and insertion/deletion loops, respectively, were less frequent. It is interesting to note in this respect that the latter premutagenic lesions are the best substrates for hMutSα in *in vitro* mismatch binding assays (34), as well as being the most efficiently corrected mispair types *in vivo* (35). It is therefore likely that although the level of hMutSα in the H-5 cells is low, it is nonetheless sufficient to mediate the correction of a significant proportion of those substrates which it binds with the highest affinity (see also below).

H-5 cells are not significantly sensitized to killing by methylating agents

Treatment of cells with simple methylating agents introduces numerous modifications into DNA. However, it could be shown that the lesion primarily responsible for the cytotoxicity of these substances is O^6-methylguanine. Resistance to methylating agents is commonly associated with overexpression of O^6-methylguanine methyltransferase (MGMT), which reverses the damage by removing methyl groups from modified guanines and thymines (18). Interestingly, mismatch repair-deficient cells have been shown to tolerate the presence of high levels of O^6-methylguanine in their DNA (36) and it has been suggested that this tolerant phenotype is due to the inability of these cells to address O^6-methylG/T and O^6-methylG/C mispairs in DNA. In mismatch repair-proficient cells, the mismatch repair system could mediate the cytotoxic effects of methylating agents by attempting to correct O^6-methylG/T and O^6-methylG/C mispairs, whereby the failure of the polymerase to find the perfect partner for the modified guanine would eventually result in the formation of a cytotoxic double-strand break (18). Like most mismatch repair-deficient lines, HCT15 cells are tolerant to alkylating agents (22). We therefore decided to test whether the hMSH6 expressing clone H-5 has become sensitized to alkylation treatment due to the restoration of mismatch repair. As shown in Figure 4a, H-5 cells were not significantly more sensitive to MNU treatment than the control H-c clone. The HCT15/DLD1 cells had been shown to express high levels of MGMT (22). In order to eliminate possible effects of the methyltransferase, we repeated the experiments in the presence of O^6-benzylguanine, a competitive inhibitor of MGMT (Figure 4b). Also under these experimental conditions, no major differences in the sensitivity of the H-c and H-5 clones to the methylating agent were observed.

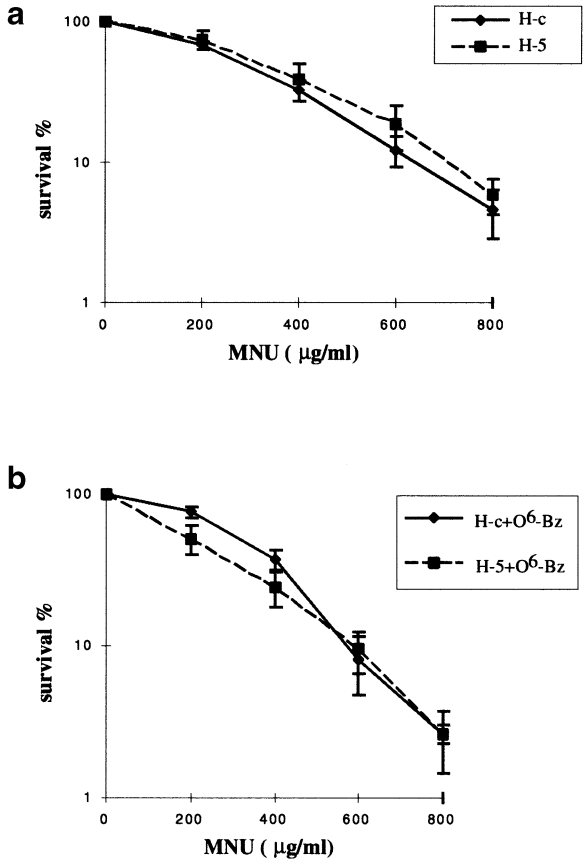

Fig. 4. Sensitivity of the H-c and H-5 cells to methylating agents. The cells were treated with MNU in the absence (**a**) or presence (**b**) of O^6-benzylguanine (see Materials and methods for details).

hMSH6 expression restores the G_2 checkpoint in H-5 cells

In the tumour cell line HCT116+3, where the mismatch repair defect was corrected by transfer of chromosome 3, MNNG treatment led to a cell cycle delay in the G_2 phase in both asynchronous and synchronized cell populations, while the

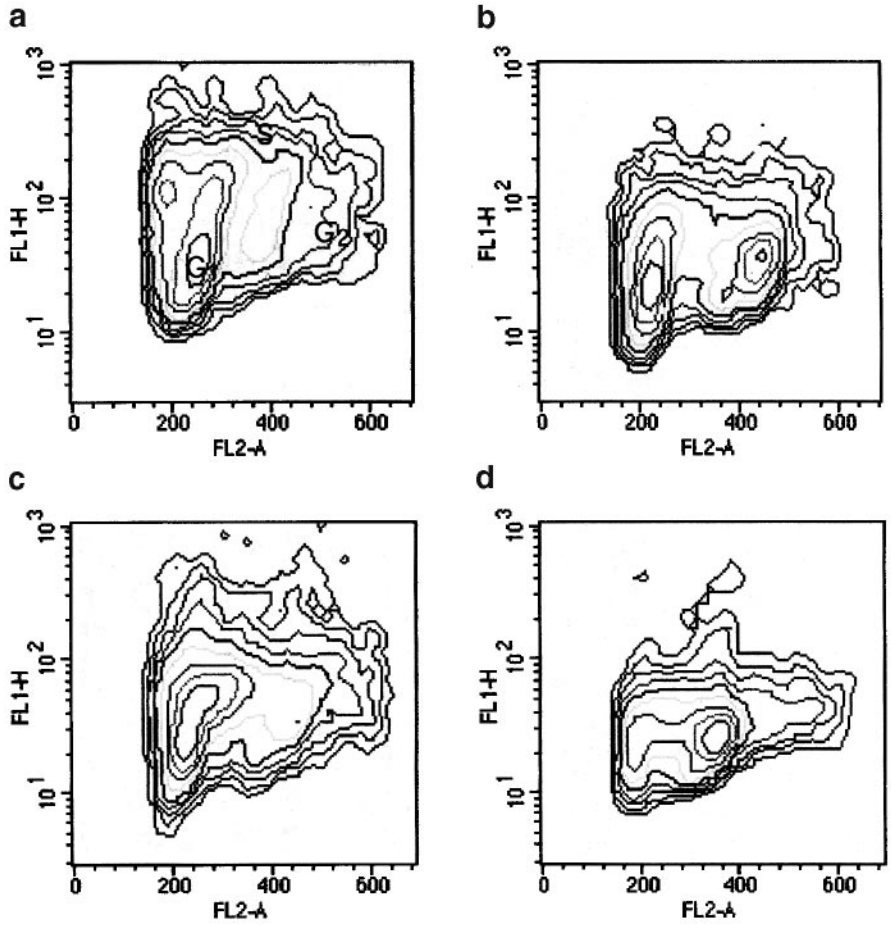

Fig. 5. Effect of MNNG treatment on the cell cycle progression of H-c and H-5 cells. The scattergrams show the cell cycle distribution of either untreated H-c (**a**) and H-5 (**c**) or MNNG-treated H-c (**b**) and H-5 (**d**) cells 15 h after release from an HU block.

parental line HCT116 was almost unaffected by the treatment (25). We decided to test whether the expression of hMSH6 in HCT15 cells had a similar effect. The cells were synchronized with HU, which blocks cells in early S phase. Following release of the HU block, the percentages of cells in the different stages of the cell cycle at various time points were studied by FACS analysis. As shown in Table IV, in the case of the control cell line H-c, most of the cells were in the S phase 2 h after HU block release. Between 7 and 12 h, most of the cells traversed S phase and entered the G_2/M phase, with the following G_1 phase appearing at 15 h post-release and a second peak of S phase cells at 19 h. A similar progression was observed with H-5 cells. However, following MNNG treatment, differences between the two lines emerged. Thus, the control H-c cell line displayed only a short delay in late S and G_2, with 30% of cells in S phase at 12 h and 20% in G_2/M at 15 h. A much longer delay in late S phase was observed in the treated H-5 cells, as demonstrated by the high percentages of S phase cells at 9 and 12 h. Although these cells slowly progressed to G_2/M, at 15 and 19 h post-release, >30% of the treated H-5 cells were still delayed in this phase.

Figure 5 shows the scattergrams at 15 h post-release, in which the different progression through G_2/M of H-c and H-5 cells is shown. At this time point, most of the MNNG-treated H-5 cells were delayed in late S phase and in G_2/M (Figure 5d), whereas a peak of G_1 cells is already evident in the treated control H-c cell line (Figure 5b).

Discussion

The human colon cancer line HCT15 contains truncating mutations in both alleles of the *hMSH6* gene (19). These mutations confer upon it a strong mutator phenotype, which demonstrates itself in the form of significantly elevated mutation rates (21) and instability of microsatellite sequences consisting of mononucleotide repeats (19). The line is also tolerant to methylating agents (22), its extracts lack mismatch binding activity (10) and are defective in mismatch correction (9). We have transfected these cells with a cDNA construct expressing wild-type hMSH6 and have studied the effects of expression of this mismatch repair protein on the phenotype of the resulting stable transfectants.

The first surprising finding was that the transfection efficiency with the control, insert-less vector was significantly higher than when the *hMSH6*-containing vector was employed. Thus, while the latter experiments yielded only two hMSH6-expressing clones, >200 were obtained in the control experiment. This seems to indicate that hMSH6-expressing clones were selected against.

Analysis of the H-5 clone revealed that although the hMSH6 protein could be detected in immunoblots (Figure 2a), it was present in amounts substantially lower than the endogenous hMSH2, its cognate partner in hMutSα. One reason for this low level of expression is that the pCDNA expression vector, integrated into the genome in three copies on average (data not shown), produced only ~50% as much *hMSH6* mRNA as

was detected in the control HeLa cells (Figure 1b, compare the specific signal with the intensity of the β-actin internal control). However, this should not be critical in itself, as immortalized lymphocytes from HNPCC patients with one mutated mismatch repair allele have been reported to be generally proficient in mismatch repair (37). The second explanation could be that the hMSH6 protein, even though expressed relatively efficiently, is subject to proteolytic degradation or misfolding prior to associating with hMSH2. Indeed, hMSH6 is known to be proteolytically labile. In extracts of cells mutated in hMSH2 (e.g. LoVo and HEC59), hMSH6 is present at barely detectable levels (10), suggesting that it is degraded in the absence of its partner hMSH2. Our previous studies showed that expression of hMSH6 without hMSH2 in a baculovirus system also resulted in a significant degradation of the former protein (13). Moreover, mixing of hMSH2 and hMSH6 expressed separately gave only low amounts of active hMutSα, while co-expression of the two proteins yielded the biologically active mismatch binding factor in high amounts (29), which suggests that the two polypeptides probably interact during folding. In their natural environment, the two genes are co-localized on chromosome 2p16 and it is likely that their expression is co-regulated, thus ensuring effective heterodimerization. This hypothesis is supported by the reports that transfer of chromosome 2 into HCT15 cells (33) resulted in a substantial correction of the mutator phenotype. The third possibility concerns the fact that hMSH6 competes for hMSH2 with another MutS homologue, hMSH3. Under normal circumstances, hMSH3 appears to be expressed at low levels and therefore the relative ratio of the hMutSα and hMutSβ heterodimers favours the former species by a substantial margin (16). However, due to the absence of hMSH6 in HCT15 cells, hMSH3 should be able to interact with hMSH2 more successfully. Indeed, hMutSβ levels in these cells have been reported to be elevated ~3-fold (16). Although expression of hMSH6 would be expected to decrease hMutSβ levels, this apparently failed to happen: the relative quantities of hMSH2 and hMSH3 in extracts of H-5 cells were similar to those detected in the control H-c line, at least as judged by immunoblotting (data not shown). We must therefore consider the possibility that expression of *hMSH6* mRNA from the pCDNA vector did not fully satisfy the criteria necessary for successful translation of the protein and for its successive heterodimerization with hMSH2.

Although present at low levels, the amount of active hMutSα in the extracts of H-5 cells was nonetheless sufficient to substantially restore mismatch binding activity (Figure 2b) and mismatch repair (Figure 3a). Most importantly, expression of wild-type hMSH6 in these cells greatly alleviated microsatellite instability at the poly(A) marker BAT26 (Table I). It was therefore somewhat surprising to discover that mutation rates, measured at the *HPRT* locus, were reduced only 3-fold (Table II) and that sensitivity of the hMSH6-expressing clone H-5 to MNU was not significantly different from the H-c control (Figure 4). How could this apparent discrepancy be explained? In our opinion, the underlying reason for these inconsistencies is the low level of hMutSα expression, coupled with the substrate specificity of this heterodimeric mismatch recognition factor. *In vitro* binding studies, carried out with purified native (38) and recombinant (13) hMutSα demonstrated that the preferred substrate is an IDL of one extrahelical nucleotide, followed by the G/T mispair. Flanking sequences also appear to play an important role in the efficiency of substrate recognition, whereby IDLs appear to be most efficiently recognized in the context of repeated motifs (39). As the dissociation constant of hMutSα with respect to the G/T oligonucleotide substrate is in the low nanomolar range (29,40), we were able to detect mismatch binding activity in the extracts of H-5 cells despite low protein amounts (Figure 2b). A similar argument applies for the *in vitro* mismatch correction experiments, which were carried out with substrates efficiently recognized by hMutSα (Figure 4). Even lower concentrations of hMutSα are required for efficient recognition of single nucleotide IDLs, which are the underlying cause of microsatellite instability in hMSH6-deficient cells. Correspondingly, the poly(A) tract of the BAT26 marker was stabilized in H-5 cells.

In contrast to microsatellites, spontaneous mutations arising in a gene such as *HPRT* are highly heterogeneous, including all types of base/base mispairs and frameshifts. Some of these will be good substrates for hMutSα and these might be expected to be corrected even in the presence of low levels of the factor. Other mispairs and, possibly, also frameshifts outside microsatellites might not be bound by hMutSα sufficiently well in order to initiate the mismatch correction process. As shown in Table III, transition mutations, which result from G/T or A/C mispairs, were down by 50% in H-5 cells, while transversions, due to either G/A, or C/T mismatches, both known to be poorly corrected *in vivo* (35), were elevated.

Restoration of sensitivity to methylating agents such as MNU or MNNG would also be expected to be affected by hMutSα concentration. The cytotoxic effects of methylating agents are probably mediated by two distinct pathways. One of these is most likely linked to abortive attempts of the mismatch repair system to correct O^6-methylG/T and O^6-methylG/C mispairs arising during replication of methylated DNA (18), whereby two concurrent mismatch repair events in close proximity may cause a double-strand break. Recent *in vitro* studies demonstrated that these mispairs are indeed recognized by hMutSα (41). However, as its affinity for O^6-methylG/T and O^6-methylG/C is substantially lower than for the G/T mispair, the majority of these methylated lesions would most likely remain unrecognized unless the cells expressed high concentrations of the mismatch binding factor. As this is clearly not the case for the H-5 line described here, its sensitivity to alkylating agents is similar to the control H-c line. The second response to DNA alkylation, or indeed to DNA damage in general, is the deployment of a cell cycle checkpoint, which allows the cell to repair the damage before proceeding with DNA replication and/or mitosis. Such a delay in cell cycle progression was documented in the mismatch repair-deficient cell line HCT116, which failed to arrest following treatment with methylating agents (25), but in which this G_2 delay was restored when the repair defect was corrected by the transfer of chromosome 3, which carries a wild-type copy of the *hMLH1* gene. The ability of mismatch repair proteins to signal to the apoptotic machinery was further documented for the closely related cell lines MT1 and TK6 (42). Treatment of the latter, mismatch repair-proficient cells with alkylating agents resulted in the elevation of p53 and p21 levels. No similar increase was observed in MT1 cells, which are mutated in *hMSH6*. As treatment of both lines with etoposide, an inhibitor of topoisomerase II, activated p53 and p21 in both lines, we concluded that p53 was wild-type in MT1 cells and that their failure to activate a p53 response following alkylation treatment was due to the absence of hMutSα-mediated damage detection. If we accept that mis-

match repair proteins are involved in DNA damage signalling to the apoptotic machinery or to the cell cycle checkpoint control, this effect could be mediated by only a few molecules, which might stall the replication fork by remaining bound at O^6-methylG/T or O^6-methylG/C mispairs and thus bring about a cell cycle arrest or delay. This hypothesis is supported by the data presented in Table IV and Figure 5, where the stably transfected H-5 line can be seen to be delayed in the late S/G_2 stage of the cell cycle following MNNG treatment, while the control H-c clone progressed with only a short delay.

Mismatch repair deficiency was linked with a multitude of phenotypic traits, ranging from microsatellite instability to tolerance to alkylating agents. Earlier studies demonstrated that transfer of chromosome 3 into hMLH1-deficient line HCT116 (43) or of chromosome 2 into HCT15 and DLD1 cells (33), both lacking hMSH6, could bring about an almost total reversion of the mutator phenotype. However, the caveat of these studies was that whole chromosomes carry many genes and thus that the correction effect could not be unambiguously assigned to a single gene. Recently, Risinger *et al*. (44) succeeded in overexpressing *hPMS2* cDNA in HEC-1-A cells and succeeded in restoring the repair of IDLs but not of base/base mismatches. This partial phenotypic correction could be explained by the discovery that these cells also harbour, in addition to the mutated *hPMS2*, a mutated *hMSH6* gene. We now show that expression of hMSH6 in the HCT15 cell line also resulted in only a partial reversion of its numerous phenotypic traits. Unlike in the case of HEC-1-A cells, however, this incomplete correction was most likely not caused by the presence of a mutation in a second mismatch repair gene. Rather, due to the low level of expression of the transgenic protein, the observed effects were only small in some instances. However, the reversion trend unambiguously confirmed the association of the *hMSH6* mismatch repair gene malfunction with mononucleotide repeat instability, elevated mutation rate and the G_2 cell cycle checkpoint.

Acknowledgements

We are indebted to Tom Kunkel for the generous gift of the HCT15 line and of the M13 mp2 phage, to Paola Delmastro for the anti-hMSH6 monoclonal antibodies and to Primo Schär for helpful discussions and for critical reading of the manuscript. This work was supported in part by the Swiss National Science Foundation and by the Julius Müller-Stiftung.

References

1. Marra,G. and Boland,C.R. (1996) DNA repair and colorectal cancer. *Gastroenterol. Clin. North Am.*, **25**, 755–772.
2. Jiricny,J. (1996) Mismatch repair and cancer. *Cancer Surv.*, **28**, 47–68.
3. Kolodner,R.D. (1995) Mismatch repair: mechanisms and relationship to cancer susceptibility. *Trends Biochem. Sci.*, **20**, 397–401.
4. Modrich,P. and Lahue,R. (1996) Mismatch repair in replication fidelity, genetic recombination, and cancer biology. *Annu. Rev. Biochem.*, **65**, 101–133.
5. Modrich,P. (1991) Mechanisms and biological effects of mismatch repair. *Annu. Rev. Genet.*, **25**, 229–253.
6. Ciotta,C., Ceccotti,S., Aquilina,G., Humbert,O., Palombo,F., Jiricny,J. and Bignami,M. (1998) Increased somatic recombination in methylation tolerant human cells with defective DNA mismatch repair. *J. Mol. Biol.*, **276**, 705–719.
7. Perucho,M. (1996) Cancer of the microsatellite mutator phenotype. *Biol. Chem.*, **377**, 675–684.
8. Fink,D., Aebi,S. and Howell,S.B. (1998) The role of DNA mismatch repair in drug resistance. *Clin. Cancer Res.*, **4**, 1–6.
9. Drummond,J.T., Li,G.M., Longley,M.J. and Modrich,P. (1995) Isolation of an hMSH2-p160 heterodimer that restores DNA mismatch repair to tumor cells. *Science*, **268**, 1909–1912.
10. Palombo,F., Gallinari,P., Iaccarino,I., Lettieri,T., Hughes,M., D'Arrigo,A., Truong,O., Hsuan,J.J. and Jiricny,J. (1995) GTBP, a 160-kilodalton protein essential for mismatch-binding activity in human cells. *Science*, **268**, 1912–1914.
11. Acharya,S., Wilson,T., Gradia,S., Kane,M.F., Guerrette,S., Marsischky,G.T. and Fishel,R. (1996) hMSH2 forms specific mispair-binding complexes with hMSH3 and hMSH6. *Proc. Natl Acad. Sci. USA*, **93**, 13629–13634.
12. Li,G.M. and Modrich,P. (1995) Restoration of mismatch repair to nuclear extracts of H6 colorectal tumor cells by a heterodimer of human MutL homologs. *Proc. Natl Acad. Sci. USA*, **92**, 1950–1954.
13. Palombo,F., Iaccarino,I., Nakajima,E., Ikejima,M., Shimada,T. and Jiricny,J. (1996) hMutSβ, a heterodimer of hMSH2 and hMSH3, binds to insertion/deletion loops in DNA. *Curr. Biol.*, **6**, 1181–1184.
14. Risinger,J.I., Umar,A., Boyd,J., Berchuck,A., Kunkel,T.A. and Barrett,J.C. (1996) Mutation of MSH3 in endometrial cancer and evidence for its functional role in heteroduplex repair. *Nature Genet.*, **14**, 102–105.
15. Marra,G., Iaccarino,I., Lettieri,T., Roscilli,G., Delmastro,P. and Jiricny,J. (1998) Mismatch repair deficiency associated with overexpression of the MSH3 gene. *Proc. Natl Acad. Sci. USA*, **95**, 8568–8573.
16. Genschel,J., Littman,S.J., Drummond,J.T. and Modrich,P. (1998) Isolation of MutSbeta from human cells and comparison of the mismatch repair specificities of MutSbeta and MutSalpha. *J. Biol. Chem.*, **273**, 19895–19901.
17. Ionov,Y., Peinado,M.A., Malkhosyan,S., Shibata,D. and Perucho,M. (1993) Ubiquitous somatic mutations in simple repeated sequences reveal a new mechanism for colonic carcinogenesis. *Nature*, **363**, 558–561.
18. Karran,P. and Bignami,M. (1994) DNA damage tolerance, mismatch repair and genome instability. *BioEssays*, **16**, 833–839.
19. Papadopoulos,N., Nicolaides,N.C., Liu,B. *et al*. (1995) Mutations of GTBP in genetically unstable cells. *Science*, **268**, 1915–1917.
20. Bhattacharyya,N.P., Skandalis,A., Ganesh,A., Groden,J. and Meuth,M. (1994) Mutator phenotypes in human colorectal carcinoma cell lines. *Proc. Natl Acad. Sci. USA*, **91**, 6319–6323.
21. Bhattacharyya,N.P. and Meuth,M. (1995) Molecular analysis of mutations in mutator colorectal carcinoma cell lines. *Hum. Mol. Genet.*, **4**, 2057–2064.
22. Branch,P., Hampson,R. and Karran,P. (1995) DNA mismatch binding defects, DNA damage tolerance, and mutator phenotypes in human colorectal carcinoma cell lines. *Cancer Res.*, **55**, 2304–2309.
23. da Costa,L.T., Liu,B., el Deiry,W. *et al*. (1995) Polymerase delta variants in RER colorectal tumours. *Nature Genet.*, **9**, 10–11.
24. Schaaper,R.M. (1988) Mechanisms of mutagenesis in the *Escherichia coli* mutator mutD5: role of DNA mismatch repair. *Proc. Natl Acad. Sci. USA*, **85**, 8126–8130.
25. Hawn,M.T., Umar,A., Carethers,J.M., Marra,G., Kunkel,T.A., Boland,C.R. and Koi,M. (1995) Evidence for a connection between the mismatch repair system and the G2 cell cycle checkpoint. *Cancer Res.*, **55**, 3721–3725.
26. Sambrook,J., Fritsch,E. and Maniatis,T. (1989) *Molecular Cloning: A Laboratory Manual*, 2nd Edn. Cold Spring Harbor Laboratory Press, Cold Spring Harbor, NY.
27. Nicolaides,N.C., Palombo,F., Kinzler,K.W., Vogelstein,B. and Jiricny,J. (1996) Molecular cloning of the N-terminus of GTBP. *Genomics*, **31**, 395–397.
28. Dignam,J.D., Martin,P.L., Shastry,B.S. and Roeder,R.G. (1983) Eukaryotic gene transcription with purified components. *Methods Enzymol.*, **101**, 582–598.
29. Iaccarino,I., Marra,G., Palombo,F. and Jiricny,J. (1998) hMSH2 and hMSH6 play distinct roles in mismatch binding and contribute differently to the ATPase activity of hMutS-alpha. *EMBO J.*, **17**, 2677–2686.
30. Bradford,M.M. (1976) A rapid and sensitive method for the quantitation of microgram quantities of protein utilizing the principle of protein–dye binding. *Anal. Biochem.*, **72**, 248–254.
31. Aquilina,G., Ceccotti,S., Martinelli,S., Hampson,R. and Bignami,M. (1998) *N*-(2-chloroethyl)-*N′*-cyclohexyl-*N*-nitrosourea sensitivity in mismatch repair-defective human cells. *Cancer Res.*, **58**, 135–141.
32. Maquat,L.E. (1995) When cells stop making sense: effects of nonsense codons on RNA metabolism in vertebrate cells. *RNA*, **1**, 453–465.
33. Umar,A., Koi,M., Risinger,J.I., Glaab,W.E., Tindall,K.R., Kolodner,R.D., Boland,C.R., Barrett,J.C. and Kunkel,T.A. (1997) Correction of hypermutability, *N*-methyl-*N′*-nitro-*N*-nitrosoguanidine resistance, and defective DNA mismatch repair by introducing chromosome 2 into human tumor cells with mutations in MSH2 and MSH6. *Cancer Res.*, **57**, 3949–3955.
34. Holmes,J.Jr, Clark,S. and Modrich,P. (1990) Strand-specific mismatch correction in nuclear extracts of human and *Drosophila melanogaster* cell lines. *Proc. Natl Acad. Sci. USA*, **87**, 5837–5841.
35. Brown,T.C. and Jiricny,J. (1988) Different base/base mispairs are corrected with different efficiencies and specificities in monkey kidney cells. *Cell*, **54**, 705–711.

36. Branch,P., Aquilina,G., Bignami,M. and Karran,P. (1993) Defective mismatch binding and a mutator phenotype in cells tolerant to DNA damage. *Nature*, **362**, 652–654.
37. Parsons,R., Li,G.M., Longley,M., Modrich,P., Liu,B., Berk,T., Hamilton,S.R., Kinzler,K.W. and Vogelstein,B. (1995) Mismatch repair deficiency in phenotypically normal human cells. *Science*, **268**, 738–740.
38. Hughes,M.J. and Jiricny,J. (1992) The purification of a human mismatch-binding protein and identification of its associated ATPase and helicase activities. *J. Biol. Chem.*, **267**, 23876–23882.
39. Macpherson,P., Humbert,O. and Karran,P. (1998) Frameshift mismatch recognition by the human MutS alpha complex. *Mutat. Res.*, **408**, 55–66.
40. Gradia,S., Acharya,S. and Fishel,R. (1997) The human mismatch recognition complex hMSH2–hMSH6 functions as a novel molecular switch. *Cell*, **91**, 995–1005.
41. Duckett,D.R., Drummond,J.T., Murchie,A.I., Reardon,J.T., Sancar,A., Lilley,D.M. and Modrich,P. (1996) Human MutSalpha recognizes damaged DNA base pairs containing O6-methylguanine, O4-methylthymine, or the cisplatin–d(GpG) adduct. *Proc. Natl Acad. Sci. USA*, **93**, 6443–6447.
42. D'Atri,S., Tentori,L., Lacal,P.M., Graziani,G., Pagani,E., Benincasa,E., Zambruno,G., Bonmassar,E. and Jiricny,J. (1998) Involvement of the mismatch repair system in temozolomide-induced apoptosis. *Mol. Pharmacol.*, **54**, 334–341.
43. Koi,M., Umar,A., Chauhan,D.P., Cherian,S.P., Carethers,J.M., Kunkel,T.A. and Boland,C.R. (1994) Human chromosome 3 corrects mismatch repair deficiency and microsatellite instability and reduces *N*-methyl-*N′*-nitro-*N*-nitrosoguanidine tolerance in colon tumor cells with homozygous hMLH1 mutation. *Cancer Res.*, **54**, 4308–4312.
44. Risinger,J.I., Umar,A., Glaab,W.E., Tindall,K.R., Kunkel,T.A. and Barrett,J.C. (1998) Single gene complementation of the hPMS2 defect in HEC-1-A endometrial carcinoma cells. *Cancer Res.*, **58**, 2978–2981.

Received September 23, 1998; revised and accepted November 12, 1998